Anomalous relaxation in fractal structures

Susumu Fujiwara and Fumiko Yonezawa
Department of Physics, Keio University, 3-14-1 Hiyoshi, Kohoku-ku, Yokohama 223, Japan
(Received 30 September 1994)

For the purpose of studying some interesting properties of anomalous relaxation in fractal structures, we carry out Monte Carlo simulations of random walks on two-dimensional fractal structures (Sierpinski carpets with different cutouts and site-percolation clusters in a square lattice at the critical concentration). We find that the relaxation is of the Cole-Cole type [J. Chem. Phys. **9**, 341 (1941)] which is one of the empirical laws of anomalous relaxation. Scaling properties are found in the relaxation function as well as in the particle density. We also find that, in structures with almost the same fractal dimension, relaxation in structures with dead ends is slower than that in structures without them. This paper ascertains that the essential aspects of the anomalous relaxation due to many-body effects can be explained in the framework of the one-body model.

PACS number(s): 61.20.Lc, 47.53.+n, 61.20.Ja

I. INTRODUCTION

Since the 19th century, the anomalous relaxation, which is characterized by a nonexponential relaxation function, has been observed in phenomena such as the viscoelastic response of solids and the strain recovery in polymers [1]. Recently, state-of-the-art experimental techniques have made it possible to measure several physical properties related to anomalous relaxation or slow dynamics in many disordered systems including supercooled liquids [2,3], spin glasses [4], and amorphous materials [1,5,6]. Most of the experimental data concerning the anomalous relaxation have so far been described in terms of empirical laws such as (i) the Cole-Cole form of the complex susceptibility $\chi(\omega)$ [7],

$$\chi(\omega) = \frac{1}{1 + (-i\omega/\omega_{\max})^{\alpha}}, \tag{1}$$

where ω is the frequency, $\omega_{\max}$ is the frequency at which the imaginary part of the complex susceptibility $\chi''(\omega)$ becomes maximum, and the parameter α satisfies $0 < \alpha \leq 1$, and (ii) the stretched-exponential form of the relaxation function [8]

$$F(t) = \exp\left[-(t/\tau)^{\beta}\right], \tag{2}$$

where t denotes time, τ is the relaxation time, and the parameter β falls in the region $0 < \beta \leq 1$. The relation between the complex susceptibility $\chi(\omega)$ and the relaxation function $F(t)$ is described by [9]

$$\chi(\omega) = 1 + i\omega \int_0^{\infty} e^{i\omega t} F(t) dt. \tag{3}$$

Note that the characteristic feature of the Cole-Cole type is that the shape of $\chi''(\omega)$ in the log-log plot is symmetric with respect to $\omega_{\max}$. On the other hand, it is asymmetric in the case of the stretched-exponential type. When $\alpha = \beta = 1$, the relaxation process is exponential (Debye relaxation). Although anomalous relaxation has been observed in a wide variety of physical quantities, its mechanism has not yet been fully understood.

The motivation of our work is to explain, in the framework of a simple model, anomalous structural relaxation phenomena which are essentially the results of many-body effects. In a many-particle system, the density autocorrelation function is considered to be the relaxation function and is measured by neutron scattering experiments. Instead of dealing with a many-particle system as it is, we propose that the essential aspects of many-body effects can be realized by applying geometrical constraints to the movement of one particle. In other words, we approximate the movement of a particle under the influence of many-body effects by the movement of one particle in a restricted geometry [10,11]. In this framework of a one-body picture, the characteristic function of a position vector corresponds to the relaxation function.

We study random walks in spaces of fractal dimensions. Here we use the word "fractal" to express that the system under consideration has the following two properties: (i) self-similarity and (ii) the fractional dimension. By Monte Carlo (MC) simulations and analytical study of random walks in structures of fractal dimensions, we demonstrate that the relaxation becomes anomalous because of the restricted geometry for one particle.

Calculations are carried out of the following physical quantities: (i) the relaxation function $F(k,t)$, (ii) the complex susceptibility $\chi(k,\omega)$, (iii) the particle density $G(r,t)$, (iv) the mean square displacement (MSD) $R(t)$, and (v) the non-Gaussian parameter (NGP) [12] $A(t)$.

This article is organized as follows. In Sec. II we describe in detail our model for anomalous structural relaxation phenomena. Our results obtained by MC simulations are presented in Sec. III. Analytical studies based on scaling arguments are represented in Sec. IV. In Sec. V a summary and a discussion are given.

II. MODEL

Suppose we have a system in which the density of particles is so high that the motion of a particle is consider-

ably restricted because of the existence of other particles. In this system a particle cannot move as it pleases [Fig. 1(a)]. Although many-body effects are expected to play important roles for structural relaxation in this system, it is interesting to clarify to what extent we can describe the essential aspects of anomalous relaxation in the framework of a one-body picture. We take many-body effects into account in terms of the geometrical constraint for a particle which walks at random [10,11] [Fig. 1(b)].

In this paper, we study the structural relaxation in fractal structures. We consider two types of structures with fractal dimensions: (i) structures without dead ends and (ii) structures with dead ends. As the first type we choose the two-dimensional (2D) Sierpinski carpets (SCs) with a central cutout [13] [Fig. 2(a)]. The fractal dimension of the 2D SCs is $d_f = \ln(b^2 - l^2)/\ln b$, where b is the system size and l is the hole size. The fractal dimension d_f is defined by

$$d_f \equiv \frac{\ln V}{\ln L} = D_0 \frac{\ln V}{\ln V_0}, \tag{4}$$

where V is the volume of the fractal structure and D_0, L, and V_0 are, respectively, the dimension, the linear dimension, and the volume of the space in which the fractal structure is placed. As the second type we choose the 2D site-percolation clusters on a square lattice at the critical concentration $p_c = 0.592\,745(2)$ [14,15] [Fig. 2(b)], for which the fractal dimension is known to be $d_f = 91/48 \approx 1.896$ [14].

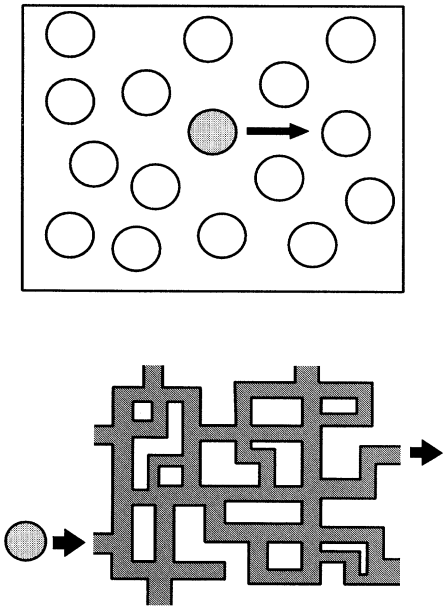

FIG. 1. (a) Schematic illustration of a system in which the density of particles is so high that the motion of a particle is considerably restricted because of the existence of other particles. (b) Schematic illustration of our model in which we take many-body effects into account in terms of the geometrical constraint for a particle which performs a random walk.

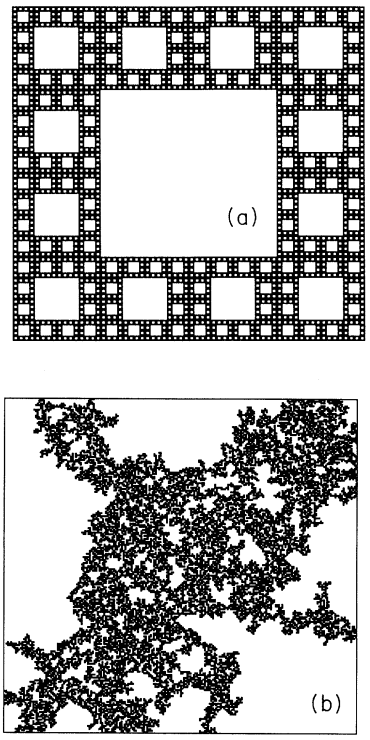

FIG. 2. (a) The 2D Sierpinski carpet of four stages with $b = 4$, $l = 2$. The fractal dimension d_f is $d_f \approx 1.7925$. (b) An example of the 2D site-percolation clusters on a square lattice at the critical concentration. The fractal dimension is $d_f = 91/48 \approx 1.896$.

III. MONTE CARLO SIMULATIONS

A. Algorithm

Our MC simulations are designed in such a way that when the dice tells a random walker to walk into a wall, he or she remains unmoved for one time step. Periodic boundary conditions and mirror boundary conditions are used for the Sierpinski structures and the percolation clusters, respectively, to remove the influence of boundaries. The self-similarity of the system holds when the area where a random walker moves is much smaller than the size of the system.

The system sizes for the 2D SCs are 729^2 ($b = 3, l = 1$), 1024^2 ($b = 4, l = 2$), and 625^2 ($b = 5, l = 1$ and $b = 5, l = 3$). The system size for the 2D percolation clusters is 400^2. The number of samples is 2×10^5 (in the case of the 2D percolation clusters, 10^4 samples on each of 20 percolation clusters). The time step of the MC simulations is 10^5.

B. Random walk on a square lattice

In our model, the relaxation function $F(k,t)$ is the characteristic function of the random variable $(\mathbf{r}(t) - \mathbf{r}(0))$:

$$F(k,t) = \left\langle e^{i\mathbf{k}\cdot(\mathbf{r}(t)-\mathbf{r}(0))} \right\rangle, \tag{5}$$

where $\mathbf{k}$ is the wave number vector, $k = |\mathbf{k}|$, $\mathbf{r}(t)$ is the position vector of a particle at time t, and the angular brackets denote the sample average. We choose $\mathbf{k} = (1,1)$ as the direction of $\mathbf{k}$.

For the sake of reference, we first carry out MC simulations of random walks on a square lattice. From a detailed analysis of the results of our simulations, we see that the relaxation function is described by the exponential function of the form [Fig. 3(a)]

$$F(k,t) = \exp\left(-\frac{t}{\tau}\right), \tag{6}$$

where the relaxation time τ is determined by the value of t at which $F(k,t) = e^{-1}$. Note that τ varies from wave number to wave number. In Fig. 3(b), the relaxation functions $F(k,t)$ for different k values are plotted after being scaled by respective τ values. We show the dependence of τ on k in Fig. 4. The solid line represents $\tau = 4k^{-2}$.

In the discussion of relaxation, it is also important to study the behavior of the imaginary part of the complex susceptibility, as noted at the beginning of Sec. I. It is easy to see from Eq. (3) that the Cole-Cole relaxation [Eq. (1)] with $\omega_{\max} = 1/\tau$ and $\alpha = 1$ is derived once the characteristic function $F(k,t)$ obeys the exponential decay, which corresponds to the case of $\beta = 1$ in Eq. (2). It is clear from Eq. (1) that $\chi''(\omega)$ has a peak at

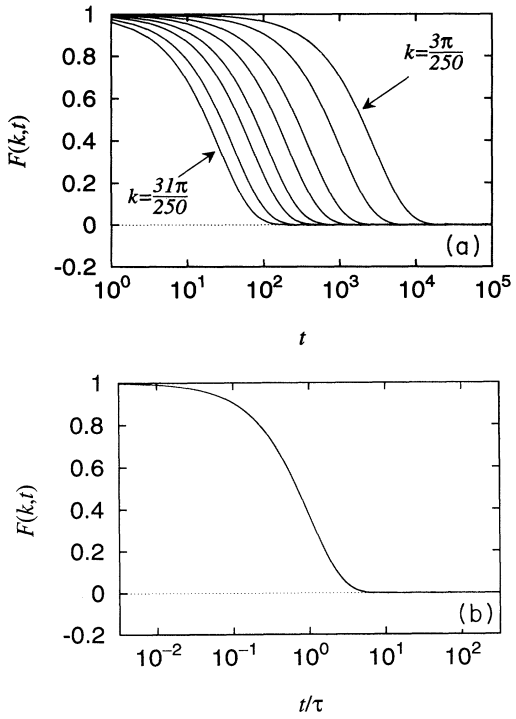

FIG. 3. (a) $F(k,t)$ vs $\log t$ for various values of k ($k = n\pi/250$, $n = 3,5,8,11,15,19,25,31$) and (b) the master curve to which $F(k,t)$ for various values of k are scaled in the case of square lattice. The solid curve represents the exponential function.

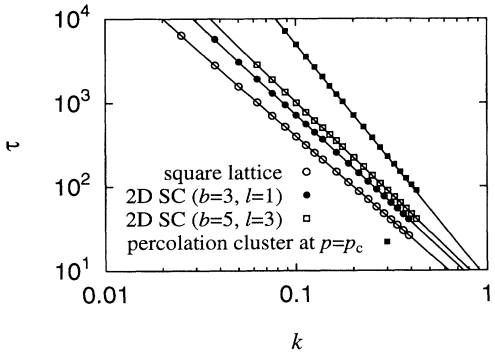

FIG. 4. $\log\tau$ vs $\log k$ for the square lattice (open circles), the 2D SC with $b = 3, l = 1$ (filled circles) and $b = 5, l = 3$ (open squares), and the 2D percolation clusters at $p = p_c$ (filled squares). The solid line represents $\tau \propto k^{-\gamma}$ with parameters $\gamma = 2.007, 2.121, 2.210$, and 2.81, respectively, obtained by the least-squares fit.

$\omega_{\max} = 1/\tau_0$, which happens to be equal to $1/\tau$ in the case of the normal diffusion. This leads to the fact that $\chi''(k,\omega)$ for different k values are scaled to a master curve by scaling ω by $\omega_{\max} = 1/\tau$ and that the dependence of $\omega_{\max}$ on k is given by $\omega_{\max} = k^2/4$.

The time dependences of the MSD $R(t)$,

$$R(t) \equiv \langle(\mathbf{r}(t) - \mathbf{r}(0))^2\rangle, \tag{7}$$

and the NGP $A(t)$,

$$A(t) \equiv \frac{\langle(\mathbf{r}(t) - \mathbf{r}(0))^4\rangle}{2R^2(t)} - 1, \tag{8}$$

are for a square lattice shown by the long-dashed curves in Figs. 5 and 6, respectively. These figures show that the MSD is proportional to t and the NGP decays to zero rapidly.

We plot $2\pi r G(r,t)\sigma$ vs r/σ for several times t in Fig. 7, where $G(r,t)$ is the particle density defined by

$$G(r,t) = \langle\delta(\mathbf{r} - \mathbf{r}(t) + \mathbf{r}(0))\rangle \tag{9}$$

and σ is the square root of the MSD. The solid curve corresponds to the relation expressed by Eq. (A4) in the

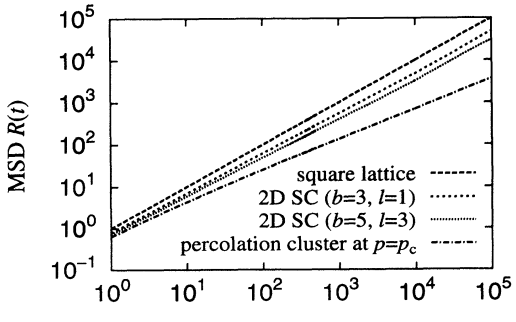

FIG. 5. The mean-square displacement $R(t)$ for the square lattice (long-dashed curve), the 2D SC with $b = 3, l = 1$ (short-dashed curve) and $b = 5, l = 3$ (dotted curve), and the 2D percolation clusters at $p = p_c$ (dot-dashed curve).

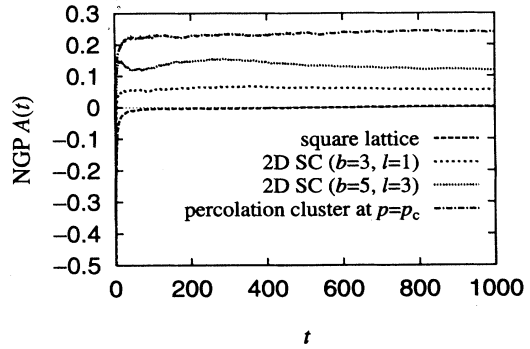

FIG. 6. The non-Gaussian parameter $A(t)$ for square lattice (long-dashed curve), the 2D SC with $b = 3, l = 1$ (short-dashed curve), and $b = 5, l = 3$ (dotted curve), and the 2D percolation clusters at $p = p_c$ (dot-dashed curve).

Appendix. We find from this figure that the scaling law for $G(r,t)$ holds. All these results presented in this subsection show that our simulations correctly reproduce the properties of the normal relaxation expected naturally for the random walks in a regular lattice such as a square lattice.

C. Random walk on fractal structures

Now let us turn to our main subject of a random walk in structures with geometrical constraints. In order to make our point clear, we start with the study of the imaginary part of the complex susceptibility $\chi''(k,\omega)$ as a function of the wave number k and the frequency ω. Although $\chi''(k,\omega)$ is related to $F(k,t)$ by Eq. (3), it is also well known that $\chi''(k,\omega)$ is derived from the relation

$$\chi''(k,\omega) = \lim_{t_{\max}\to\infty} \frac{\omega}{2t_{\max}} \left\langle \left| \int_0^{t_{\max}} \exp\left[i\mathbf{k}\cdot\mathbf{r}(t)\right] e^{i\omega t} dt \right|^2 \right\rangle . \tag{10}$$

In our analysis, we take the maximum time steps of our MC simulations as $t_{\max}$, i.e., $t_{\max} = 10^5$.

In Fig. 8 the imaginary parts of the complex susceptibility $\chi''(k,\omega)$ scaled by $\omega_{\max}$ are shown in the case of (a) the 2D SC with $b = 3, l = 1$ and (b) the 2D percolation clusters at $p = p_c$. Note that $\omega_{\max}$ is the frequency at which $\chi''(k,\omega)$ has a maximum value. From these figures, we find the following features: (i) $\chi''(k,\omega)$ for different values of k are beautifully scaled by $\omega_{\max}$. (ii) For each value of k, $\chi''(k,\omega)$ is symmetric with respect to $\omega_{\max}$ in the log-log plot, which is a characteristic feature of the Cole-Cole form. In fact, the data of our MC simulations (open and filled circles, squares, diamonds, and triangles) agree remarkably well with the solid curve, which represents the Cole-Cole form [Eq. (1)] with $\alpha = 0.954$ in Fig. 8(a) and $\alpha = 0.748$ in Fig. 8(b).

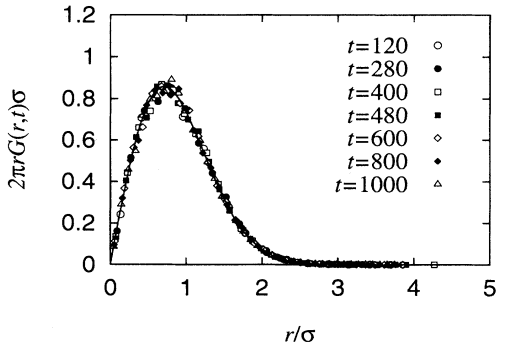

FIG. 7. $2\pi rG(r,t)\sigma$ vs r/σ for various times t in the case of the square lattice. The solid curve corresponds to the relation represented by Eq. (A4) in the Appendix.

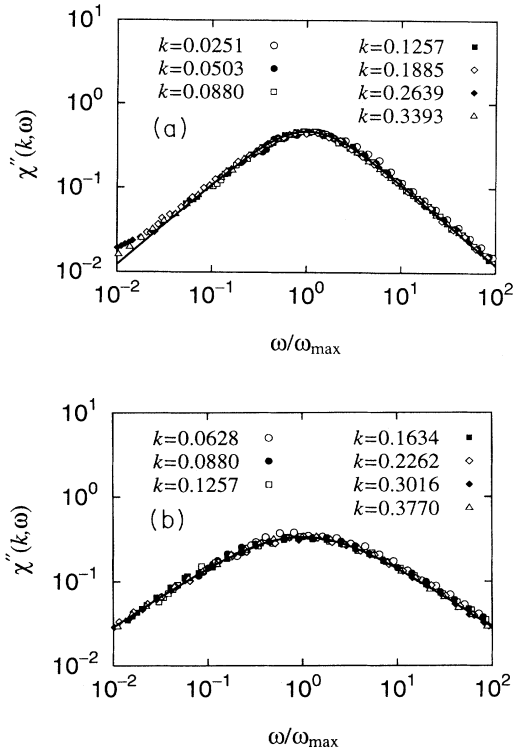

FIG. 8. $\log \chi''(k,\omega)$ vs $\log(\omega/\omega_{\max})$ for various values of k (a) in the case of the 2D SC with $b = 3, l = 1$ and (b) in the case of the 2D percolation clusters at $p = p_c$. The solid curve represents the Cole-Cole susceptibility with (a) $\alpha = 0.954$ and (b) $\alpha = 0.748$.

The parameter α depends on the fractal dimension d_f. The actual dependence of α on the normalized fractal dimension d_f/D_0 (in this case $D_0 = 2$) is presented in Fig. 9 for the 2D SCs. This figure shows that α decreases when d_f/D_0 is reduced, which reflects the fact that the smaller the fractal dimension, the slower the relaxation. The results for the 2D percolation clusters at $p = p_c$ are shown in Table I. When we compare the parameter α obtained from the 2D percolation clusters at $p = p_c$ and from the 2D SCs with $b = 3, l = 1$ at almost the same values of d_f/D_0, we find that the former is much smaller than the latter. This fact is understood in the following way. In the fractal structures with no dead ends such as the Sierpinski structures, the slowing down of the relaxation is caused by the blockings due to walls, in which case it is relatively easy for particles to find detours. On the other hand, in the fractal structures

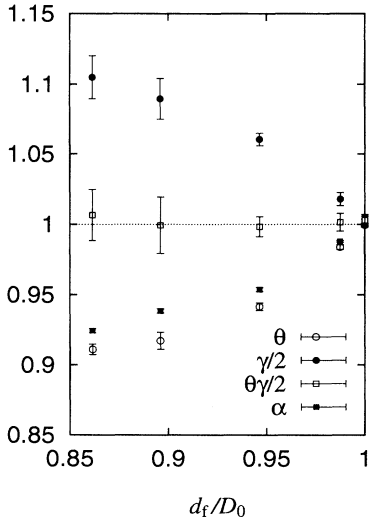

FIG. 9. Parameters vs d_f/D_0 for the 2D SC: θ (open circles), $\gamma/2$ (filled circles), $\theta \times \gamma/2$ (open squares), and α (filled squares).

such as the percolation clusters, which are characterized by a number of dead ends at various stages of hierarchy, it takes quite a long time for particles to escape from dead ends once they are trapped therein and accordingly the relaxation becomes largely slow.

The results of our simulations also show that, for each given fractal structure, the peak position of $\chi''(k,\omega)$ changes as a function of k in the form $\omega_{\max} \propto k^{\gamma}$ with $\gamma > 2$. It is interesting to remember that, as explained in Sec. III B, $\omega_{\max} \propto k^2$ for the case of the normal relaxation.

As for $F(k,t)$, the results for various k values are shown in Figs. 10(a) and 11(a) in the case of the 2D SCs with $b = 3, l = 1$ and the 2D percolation clusters at $p = p_c$, respectively.

Here it is interesting to remember the fact described in Sec. III B that for the normal relaxation the quantity $1/\omega_{\max}$ obtained from the peak position of $\chi''(k,\omega)$ defined by Eq. (1) is identical to the relaxation time τ, which is the scaling factor for the characteristic function $F(k,t)$ given by Eq. (2). Since Eq. (1) of the Cole-Cole type and Eq. (2) of the stretched-exponential type are not mutually related via the Fourier-Laplace transformation except for the case of $\alpha = \beta = 1$, our results of the Cole-Cole type anomalous relaxation in the fractal structures

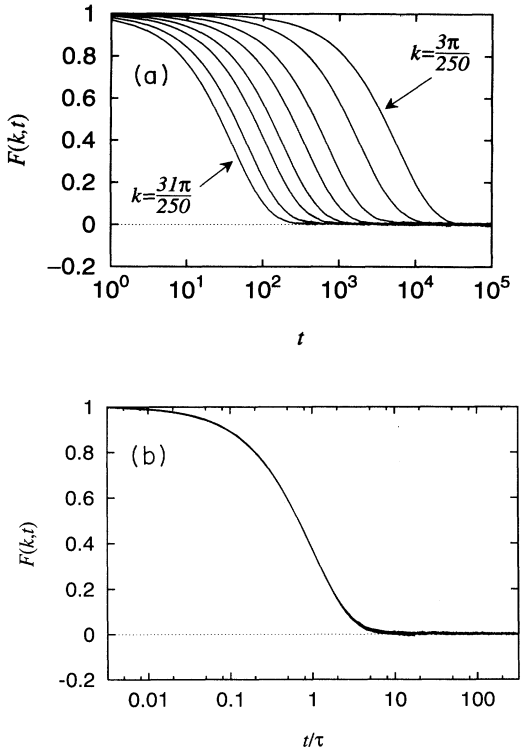

FIG. 10. (a) $F(k,t)$ vs $\log t$ for various values of k ($k = n\pi/250$, $n = 3, 5, 8, 11, 15, 19, 25, 31$) and (b) the master curve to which $F(k,t)$ for various values of k are scaled in the case of the 2D SC with $b = 3, l = 1$. The solid curve is the relaxation function of the Cole-Cole type with the parameter $\alpha = 0.954$.

never lead to the stretched-exponential form of Eq. (2) and therefore the curves shown in Figs. 10(a) and 11(a) are not of the stretched-exponential form. However, Eq. (3) indicates that, when $\chi''(\omega)$ is scaled by, say, ω_0, $F(t)$ is also scaled by $1/\omega_0$. In our case here, $\omega_0 = \omega_{\max}$ as we clarified in Figs. 8(a) and 8(b), the scaling factor for $F(k,t)$ has to be $\tau = 1/\omega_{\max}$. The results after scaling by this factor are shown in Figs. 10(b) and 11(b). In both cases, the scaling property is remarkable, especially in the region around $t = \tau$.

Since we have $\tau = 1/\omega_{\max}$, the k dependence of τ is given by

$$\tau \propto k^{-\gamma} \tag{11}$$

TABLE I. Results for the 2D SC and the 2D percolation clusters.

b	l	d_f	α	θ	γ	$\theta \times \gamma$	d_s
				2D SC			
5	1	1.975	0.988 ± 0.001	0.984 ± 0.002	2.036 ± 0.009	2.003 ± 0.013	1.940 ± 0.009
3	1	1.893	0.954 ± 0.003	0.941 ± 0.003	2.121 ± 0.009	1.997 ± 0.014	1.785 ± 0.008
4	2	1.792	0.938 ± 0.002	0.917 ± 0.006	2.179 ± 0.029	1.999 ± 0.040	1.645 ± 0.022
5	3	1.723	0.924 ± 0.003	0.911 ± 0.004	2.210 ± 0.031	2.013 ± 0.036	1.559 ± 0.022
				2D percolation clusters			
		1.896	0.748 ± 0.010	0.719 ± 0.003	2.81 ± 0.10	2.02 ± 0.08	1.35 ± 0.05

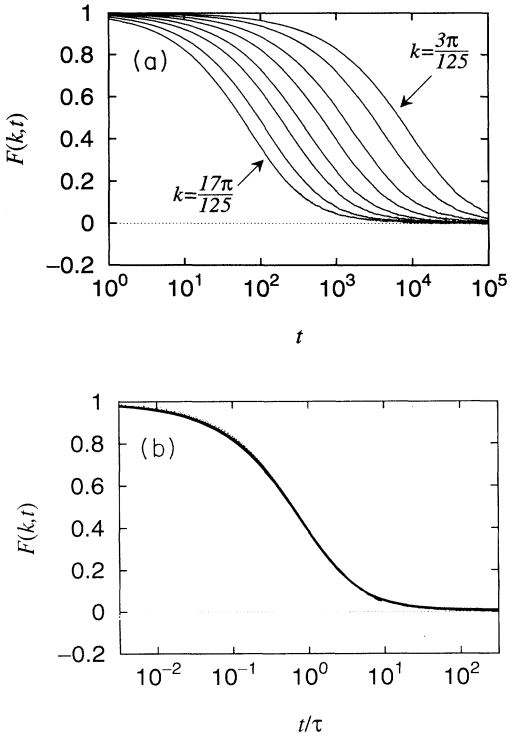

FIG. 11. (a) $F(k,t)$ vs $\log t$ for various values of k ($k = n\pi/250$, $n = 6, 8, 11, 14, 18, 22, 28, 34$) and (b) the master curve to which $F(k,t)$ for various values of k are scaled in the case of the 2D percolation clusters at $p = p_c$. The solid curve is the relaxation function of the Cole-Cole type with the parameter $\alpha = 0.748$.

with $\gamma > 2$. The values of γ are given in Table I and γ vs d_f/D_0 is plotted in the case of the 2D SCs in Fig. 9. From this figure, we find that $\gamma/2$ increases from 1 as the fractal dimension d_f/D_0 decreases from 1.

Figure 5 shows that the MSD $R(t)$ is expressed by the relation

$$R(t) \propto t^{\theta} \tag{12}$$

with $\theta < 1$, except for the case of a square lattice which has $\theta = 1$, that is, the diffusion is anomalous. From the open circles in Fig. 9, we find that θ decreases from 1 as the fractal dimension d_f/D_0 decreases from 1. We also find from Fig. 6 that, except for the long-dashed curve corresponding to a square lattice, the NGP $A(t)$ does not decay to zero but stays almost constant.

Since the particle density as defined by Eq. (9) is given by

$$G(r,t) = \frac{1}{(2\pi)^2} \int F(k,t) \exp(-i\mathbf{k}\cdot\mathbf{r})\, d\mathbf{k}, \tag{13}$$

then the MSD $R(t)$ as defined by Eq. (7) is calculated by

$$R(t) = \int r^2 G(r,t) d\mathbf{r}. \tag{14}$$

When the scaling of $F(k,t)$ holds and the relations $\tau \propto k^{-\gamma}$ and $R(t) \propto t^{\theta}$ are fulfilled, we show through a straightforward dimension analysis that

$$\theta \times \gamma/2 = 1. \tag{15}$$

As clearly judged from the open squares in Fig. 9, this relation evidently holds. Equation (15) is also significant in the sense that it relates a parameter θ concerning *diffusion* to a parameter γ concerning *relaxation*.

The above-mentioned scaling law of $F(k,t)$ in the $\mathbf{k}$ space suggests the scaling law of $G(r,t)$ in the $\mathbf{r}$ space. From Eqs. (11) and (15), $G(r,t)$ is considered to be scaled by $r \propto t^{+1/\gamma} \propto t^{\theta/2}$, that is, σ is the square root of the MSD. In fact, the scaling law of $G(r,t)$ is obviously seen in Fig. 12 for the 2D percolation clusters.

We also calculate the spectral dimension d_s, which is defined as the exponent characterizing the spectral density of states in fractal networks [16]. We can show that the spectral dimension d_s is related to other parameters through $d_s = \theta d_f$. When we use the fractal dimension d_w of random walk, d_s is expressed as $d_s = 2d_f/d_w$ because θ is related to d_w as $\theta = 2/d_w$ [17]. The value of d_s thus calculated in the case of the 2D percolation clusters at $p = p_c$ is consistent with the known value of about 4/3 drawn from the Alexander-Orbach conjecture [16] within error bars. The spectral dimensions in the case of the 2D SCs are not known exactly. For the 2D SCs with $b = 3, l = 1$, Hattori *et al.* [18] got the value $d_s^{\mathrm{POP}} = 1.721$ in the pattern-on-pattern (POP) approximation and Watanabe [19] obtained the value $d_s^{\mathrm{MK}} = 1.862$ in the Migdal-Kadanoff (MK) approximation. Our results lead to the value $d_s = 1.785 \pm 0.008$, which falls between these two approximate values d_s^{POP} and d_s^{MK}.

IV. ANALYTICAL STUDIES

A. Asymptotic forms for $F(k,t)$ and $\chi''(k,\omega)$

In this subsection, we study the asymptotic behavior of $F(k,t)$ and $\chi''(k,\omega)$ on the basis of the scaling argument for the probability density $G(r,t)$ of random walks on fractals. As $G(r,t)$ is the probability density function, $G(r,t)d\mathbf{r}$ represents the probability that we find a particle in a region between $\mathbf{r}$ and $\mathbf{r} + d\mathbf{r}$ at time t when the

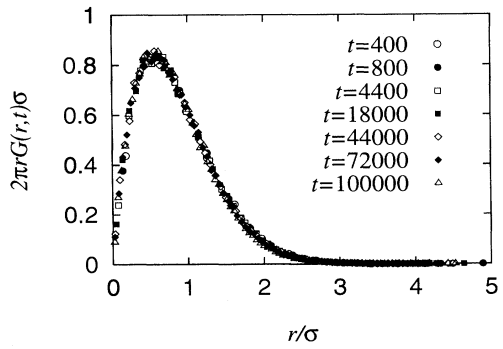

FIG. 12. $2\pi r G(r,t)\sigma$ vs r/σ for various times t in the case of the 2D percolation clusters at $p = p_c$.

particle starts from the origin $\mathbf{r} = \mathbf{0}$ at time 0. Then the probability that we find a particle in the vicinity $d\mathbf{r}$ of the origin at time t is $G(0,t)d\mathbf{r}$. The number of sites that a particle has visited after time t is proportional to the volume $R^{d_f/2}(t) \propto t^{d_f/d_w}$, where the MSD $R(t)$ has the relation $R(t) \propto t^{2/d_w}$. [In this section, we use the conventional exponent d_w (the fractal dimension of random walk) instead of θ ($\theta = 2/d_w$).] Therefore the probability of that particle returning to the origin $G(0,t)d\mathbf{r}$ is written as

$$G(0,t)d\mathbf{r} \sim \frac{1}{R^{d_f/2}} \sim t^{-d_f/d_w}. \tag{16}$$

The scaling behavior of probability densities was studied by Havlin *et al.* [20]. One expects the following scaling form for $G(r,t)$:

$$G(r,t) = \frac{r^{d_f - D_0}}{t^{d_f/d_w}} \Pi\left(\frac{r}{t^{1/d_w}}\right). \tag{17}$$

Here the $r^{d_f - D_0}$ factor comes from the scaling of the density of the fractal substrate and the factor of t^{d_f/d_w} is required because of Eq. (16). Note that $\Pi(x)$ is a function of argument x alone. The scaling factor of r, t^{1/d_w}, comes from the anomalous diffusion theory [Eq. (12)]. In the case of the 2D site-percolation clusters at $p = p_c$, $D_0 = 2$, $d_f = 91/48 \approx 1.896$ [14], and $d_w = 2.87 \pm 0.02$ [21].

The relaxation function $F(k,t)$ is written as the Fourier transform of $G(r,t)$ with respect to $\mathbf{r}$:

$$F(k,t) = \int G(r,t) e^{i\mathbf{k}\cdot\mathbf{r}} d\mathbf{r}. \tag{18}$$

When the scaling of $G(r,t)$ [Eq. (17)] holds, $F(k,t)$ is rewritten as

$$F(k,t) = \frac{2\pi}{t^{d_f/d_w}} \int_0^\infty r^{d_f-1} J_0(kr) \Pi\left(\frac{r}{t^{1/d_w}}\right) dr \tag{19}$$

$$= 2\pi \int_0^\infty R^{d_f-1} J_0\left(t^{1/d_w} kR\right) \Pi(R) dR, \tag{20}$$

where J_0 is the zeroth-order Bessel function of the first kind. From Eq. (20), it is found that $F(k,t)$ depends on k and t only through the product $t^{1/d_w}k$, that is, $F(k,t)$ shows scaling for various values of k: $F(k,t) = \tilde{F}(t/\tau)$ with $\tau \propto k^{-1/d_w}$.

First, we study the asymptotic behavior of $F(k,t)$ in the limit $t \to \infty$. When the scaling function $\Pi(x)$ is holomorphic at the origin $x = 0$, $\Pi(x)$ is expanded in Taylor's expansion as follows:

$$\Pi(x) = \Pi(0) + \frac{d\Pi(0)}{dx} x + O(x^2). \tag{21}$$

Substituting Eq. (21) into Eq. (19), we get

$$F(k,t) = \frac{2\pi}{t^{d_f/d_w}} \int_0^\infty r^{d_f-1} J_0(kr) \Pi(0) dr + O(t^{-(1+d_f)/d_w})$$

$$\sim t^{-d_f/d_w} \quad (t \to \infty). \tag{22}$$

Next, we study the asymptotic behavior of $F(k,t)$ in the limit $t \to 0$. In the case of $z \ll 1$, $J_0(z)$ is expanded as

$$J_0(z) = 1 - \frac{1}{4} z^2 + O(z^4). \tag{23}$$

From Eqs. (23) and (20), we obtain

$$F(k,t) = 2\pi \int_0^\infty R^{d_f-1} \Pi(R) \left[1 - \frac{1}{4} t^{2/d_w} k^2 R^2\right] dR + O(t^{4/d_w})$$

$$\sim 1 - t^{2/d_w} \frac{\pi k^2}{2} \int_0^\infty R^{d_f+1} \Pi(R) dR \quad (t \to 0). \tag{24}$$

Here we have used the normalization condition

$$\int G(r,t) d\mathbf{r} = 1 \tag{25}$$

in the derivation of the first term in Eq. (24).

In order to get the asymptotic forms of $\chi''(k,\omega)$ from the asymptotic forms of $F(k,t)$ [Eqs. (22) and (24)], we use the following formula:

$$\int_0^\infty e^{-st} t^{k-1} dt = \frac{\Gamma(k)}{s^k} \quad (k > 0), \tag{26}$$

where $\Gamma(k)$ is the gamma function. As a result, we find

$$\chi''(k,\omega) \sim \begin{cases} \omega^{d_f/d_w} & (\omega \ll 1/\tau) \\ \omega^{-2/d_w} & (\omega \gg 1/\tau). \end{cases} \tag{27}$$

B. Forms for $F(k,t)$ and $\chi''(k,\omega)$ in the intermediate time or frequency scale

The functional form of the scaling function $\Pi(x)$ of random walks on the 2D site-percolation clusters at $p = p_c$ on a square lattice was extensively studied by Havlin *et al.* using the exact enumeration method [20]. They assumed the following functional form for $\Pi(x)$:

$$\Pi(x) = \exp(-Ax^a) \tag{28}$$

and obtained the value of an exponent a by fitting their data,

$$a = 1.65 \pm 0.10, \tag{29}$$

where A is determined from the normalization condition for $G(r,t)$ [Eq. (25)] as

$$A = \left[\frac{2\pi}{a} \Gamma\left(\frac{d_f}{a}\right)\right]^{a/d_f}. \tag{30}$$

Substituting Eqs. (28) and (29) into Eq. (19), we get

$$F(k,t) = 2\pi \int_0^\infty R^{d_f-1} J_0\left(t^{1/d_w} kR\right) e^{-AR^a} dR. \tag{31}$$

In Fig. 13 we show the relaxation function $F(k,t)$ obtained by performing an integral in Eq. (31). From this figure we find that the scaling argument [Eq. (31)] and our MC simulations give remarkable agreement. Consequently it is ascertained that the relaxation is of the Cole-Cole type in the intermediate time scale (in this fig-

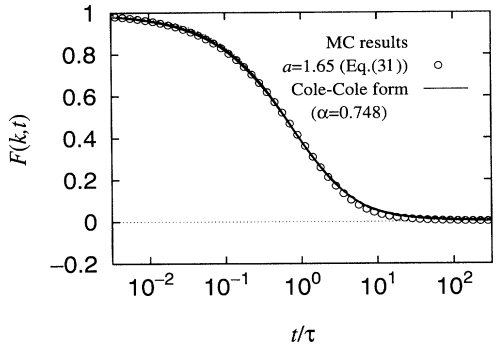

FIG. 13. $F(k,t)$ vs $\log(t/\tau)$ in the case of the 2D percolation clusters at $p = p_c$. Dots represent our MC result, open circles denote the result obtained by performing an integral in Eq. (31) with $a = 1.65$, and the solid curve is the relaxation function of the Cole-Cole type with the parameter $\alpha = 0.748$.

ure, over five decades around $t = \tau$).

Combining the result in this subsection and Eq. (27), we find

$$\chi''(k,\omega) \sim \begin{cases} \omega^{d_f/d_w}, & \omega \ll 1/\tau \\ \mathrm{Im}\dfrac{1}{1+(-i\omega\tau)^{\alpha}}, & \text{intermediate frequency} \\ \omega^{-2/d_w}, & \omega \gg 1/\tau\ . \end{cases} \tag{32}$$

A schematic illustration of $\chi''(k,\omega)$ [Eq. (32)] is shown in Fig. 14. From our MC results, we find the following relation among α and the absolute values of slopes:

$$\frac{d_f}{d_w} < \frac{2}{d_w} < \alpha. \tag{33}$$

Judging from our MC results (Sec. III) together with our scaling argument (Sec. IV), we conclude that the relaxation in fractal structures is described by the Cole-Cole form over quite a wide range in the intermediate time region around τ and in the intermediate frequency region around $\omega_{\max}$, which are the regions of interest. The deviation from the Cole-Cole relaxation appears only outside these regions.

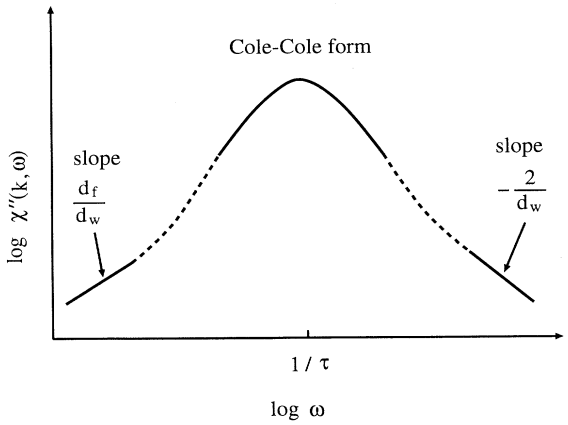

FIG. 14. Schematic illustration of $\chi''(k,\omega)$ for random walks on 2D fractals.

V. SUMMARY AND DISCUSSION

From our MC results of random walks on fractal structures and analytical studies based on the scaling argument, we have shown the following properties.

(i) The anomalous relaxation is ascribable to the restricted geometry allowed for diffusion.

(ii) The relaxation in fractal structures is of the Cole-Cole type in the intermediate time and frequency region around τ and $\omega_{\max}$, respectively, which are the regions of interest.

(iii) $F(k,t)$, $\chi(k,\omega)$, and $G(r,t)$ show scaling.

(iv) The relation $\theta \times \gamma/2 = 1$ holds between a parameter θ characterizing diffusion and a parameter γ characterizing relaxation.

(v) In structures with almost the same fractal dimension, the relaxation in structure with dead ends is slower than that in structure without them.

(vi) The spectral dimension d_s obtained by our MC simulations in the case of the 2D SCs with $b = 3, l = 1$ is between the approximate values d_s^{POP} and d_s^{MK} obtained earlier.

In this way, we have proposed and studied the model of random walks in structures with fractal dimensions on the confident expectation that our model embodies the essential aspects of the structural relaxation in many-body systems. Summarizing the above-mentioned results of ours, we assure that the present work really gives important clues to the understanding of the mechanisms of anomalous relaxation. Another possible model in the framework of one-body picture is the fractal time random walk (FTRW) in regular lattices [22]. In the FTRW model, the relaxation is also shown to be of the Cole-Cole type [22]. This fact is extremely interesting and gives us a future work on the relation between random walks in fractal structures and the FTRW in regular lattices. The anomalous relaxation of the stretched-exponential type will be realized with other types of restricted geometry [11].

It is worth mentioning that, in the recent studies of anomalous relaxation, Niklasson has studied the dielectric response of disordered materials on the basis of the generalized diffusion equation [23]. He analyzed the equation by means of the concept of fractal.

ACKNOWLEDGMENTS

The authors are grateful for valuable discussions with S. Gomi. This work was supported in part by the Grant-in-Aid for Scientific Research on Priority Areas from the Ministry of Education, Science, and Culture of Japan.

APPENDIX: CUMULANT EXPANSION OF THE RELAXATION FUNCTION

The relaxation function $F(k,t)$ is the characteristic function of the random variable $(\mathbf{r}(t) - \mathbf{r}(0))$ as defined by Eq. (5). It is shown that the probability distribution function of $(\mathbf{r}(t) - \mathbf{r}(0))$ is the particle density $G(r,t)$,

$$F(k,t) = \int G(r,t) e^{i\mathbf{k}\cdot\mathbf{r}} d\mathbf{r}. \tag{A1}$$

We can expand $F(k,t)$ in powers of k^2 (cumulant expansion) [12] as follows:

$$F(k,t) = \exp\left[\sum_{n=1}^{\infty} \frac{(ik)^n}{n!} \langle (\mathbf{r}(t) - \mathbf{r}(0))^n \rangle_c\right]. \tag{A2}$$

In the case of a two-dimensional system, we have

$$F(k,t) = \exp\left[-\frac{k^2}{4} R(t) \left(1 - \frac{k^2}{12} R(t) A(t) + \cdots\right)\right], \tag{A3}$$

where $R(t) \equiv \langle (\mathbf{r}(t) - \mathbf{r}(0))^2 \rangle$ is the mean-square displacement, $\langle (\mathbf{r}(t) - \mathbf{r}(0))^n \rangle_c$ is the nth cumulant of $(\mathbf{r}(t) - \mathbf{r}(0))$, and $A(t)$ is the non-Gaussian parameter defined by Eq. (8).

When the particle density $G(r,t)$ has a Gaussian form

$$G(r,t) = \frac{1}{2\pi R(t)} \exp\left(-\frac{r^2}{2R(t)}\right), \tag{A4}$$

the nth cumulant with $n \geq 3$ is zero. Accordingly, the relaxation function $F(k,t)$ is exponential, that is, the relaxation is of the normal Debye type:

$$F(k,t) = \exp\left(-\frac{t}{\tau}\right), \tag{A5}$$

$$\tau = 2D_0 k^{-2} = 4k^{-2}. \tag{A6}$$

[1] H. Scher, M.F. Shlesinger, and J.T. Bendler, Phys. Today **44** (1), 26 (1991).
[2] W. Götze, in *Liquids, Freezing and Glass Transition*, edited by J.-P. Hansen, D. Levesque, and J. Zinn-Justin (North-Holland, Amsterdam, 1991).
[3] J.-P. Hansen, Phys. World **4**, 32 (1991).
[4] K. Binder and A.P. Young, Rev. Mod. Phys. **58**, 801 (1986).
[5] J. Kakalios, R. A. Street, and W. B. Jackson, Phys. Rev. Lett. **59**, 1037 (1987).
[6] Y. Fujita, M. Yamaguchi, and K. Morigaki, Philos. Mag. B **69**, 57 (1994).
[7] K.S. Cole and R.H. Cole, J. Chem. Phys. **9**, 341 (1941).
[8] G. Williams and D.C. Watts, Trans. Faraday Soc. **66**, 80 (1970).
[9] R. Kubo, J. Phys. Soc. Jpn. **12**, 570 (1957).
[10] S. Fujiwara, S. Gomi, K. Morigaki, and F. Yonezawa, J. Non-Cryst. Solids **164-166**, 301 (1993).
[11] S. Fujiwara and F. Yonezawa (unpublished).
[12] J.-P. Hansen and I.R. McDonald, *Theory of Simple Liquids*, 2nd ed. (Academic, London, 1986).
[13] B.B. Mandelbrot, *The Fractal Geometry of Nature* (Freeman, San Francisco, 1982).
[14] D. Stauffer, *Introduction to Percolation Theory* (Taylor & Francis, London, 1985).
[15] R.M. Ziff and B. Sapoval, J. Phys. A **19**, L1169 (1986).
[16] S. Alexander and R. Orbach, J. Phys. Lett. **43**, 625 (1982).
[17] S. Havlin and D. Ben-Avraham, Adv. Phys. **36**, 695 (1987).
[18] K. Hattori, T. Hattori, and H. Watanabe, Phys. Rev. A **32**, 3730 (1985).
[19] H. Watanabe, J. Phys. A **18**, 2807 (1985).
[20] S. Havlin, D. Movshovitz, B. Trus, and G.H. Weiss, J. Phys. A **18**, L719 (1985).
[21] S. Havlin and D. Ben-Avraham, J. Phys. A **16**, L483 (1983); I. Majid, D. Ben-Avraham, S. Havlin, and H.E. Stanley, Phys. Rev. B **30**, 1626 (1984).
[22] S. Gomi and F. Yonezawa (unpublished).
[23] G.A. Niklasson, J. Phys. Condens. Matter **5**, 4233 (1993).